

The Esiac-10 Algebraic Computer



Kees Pronk and Piet Trimp (EEMCS Historic Collection)

Introduction

From time to time, the volunteers of the Historic Collection in the basement of the EEMCS building come across unknown equipment. In this article, we discuss one such special find: the ESIAC-10 Algebraic Computer (figure 1). We discuss the principles and operation of this analogue computer intended to solve algebraic equations such as those found in control engineering.

A short survey of the TU Delft archives has presented us with only one reference to this machine [1]. The ESIAC-10 analogue computer is mentioned in the book *Spanning* from 1998 by professor J. Davidse, but was already characterized as being overruled by the digital computers of that time. From further study, we suggest that the machine was bought by professor L.H.M. Huydts (honorary member of the ETV) around 1965.

A further literature study established that the ESIAC has been the subject of a thesis by M. L. Morgan in 1954 [2]. Around 1960 his prototype was converted into a commercial product. Several papers were devoted to the new computer to show its construction and advantages over earlier equipment [3, 4, 5]. We became aware of two publications by NASA [6, 7] showing the application domain of the machine: control theory, transfer functions, Bode (magnitude and phase vs. frequency) plots and root locus diagrams of dynamic systems.



Figure 1 The ESIAC-10 Algebraic Computer

The mathematics of dynamic systems

The application domain of the ESIAC-10 is control engineering where so-called dynamic systems are studied. Such dynamic systems can be (electric) networks or feedback systems. Mathematically, dynamic systems are characterized by their transfer function: the quotient of the output voltage and the input voltage as a function of frequency.

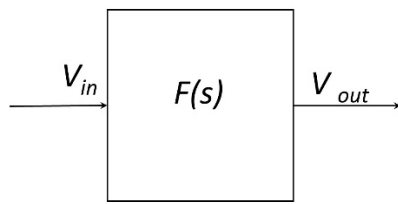


Figure 2 Transfer function of a dynamic system

The transfer function $F(s) = \frac{V_{out}}{V_{in}}$ of a dynamic system (figure 2) is given by the following formula:

$$F(s) = \frac{a_0 + a_1s + a_2s^2 + \dots + a_cs^c}{b_0 + b_1s + b_2s^2 + \dots + b_ds^d}$$

where s equals the frequency, $j\omega$ or z (as in sampled data systems).

The transfer function can be visualized as in figure 3: a vector F in the s -plane. Note that the s -plane is of infinite size and that it is not possible to 'remember' how many rotations of 2π a vector has made.

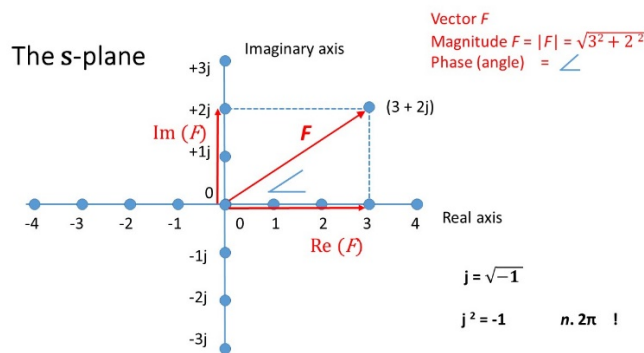


Figure 3 The s -plane showing the vector F and its real and imaginary components

The s -plane is inconvenient to use for calculating frequency and phase plots and root locus diagrams. In the next paragraph the function $F(s)$ will be factorized into entities such as poles and zeros that are meaningful to the control engineer. To construct a useful tool, the s -plane will first be converted to a rectangular log s plane, followed by three transformations: a dual network transformation, a reciprocity theorem transformation and the introduction of a limitation of the boundaries of the infinite s -plane.

Factorization

This formula of the transfer function can be factored in two ways. Due to space restrictions we do not present the second derivation but restrict ourselves to give the outcome of the second factorization in the footnote below¹.

¹ In the alternative factoring we will find the following equation:

$$F(s) = K_1 s^{n_0} \frac{(s-s_1)^{n_1}(s-s_3)^{n_3} \dots}{(s-s_2)^{n_2}(s-s_4)^{n_4} \dots} \quad \text{where } K_1 = \frac{a_c}{b_d}$$

Using $K_2 = \frac{a_0}{b_0}$ we find the following equation:

$$F(s) = K_2 s^{n_0} \frac{\left(1 - \frac{s}{s_1}\right)^{n_1} \left(1 - \frac{s}{s_3}\right)^{n_3} \dots}{\left(1 - \frac{s}{s_2}\right)^{n_2} \left(1 - \frac{s}{s_4}\right)^{n_4} \dots}$$

or alternatively: $F(s) = K_2 s^{n_0} \prod_i (1 - s/s_i)^{n_i}$

where s_1, s_3, \dots are called the zeros of the equation, s_2, s_4, \dots are called the poles of the equation and n_0 is the number of zeros minus the number of poles existing at the origin of the diagram. In these formulas all the s_i 's are complex numbers. The meaning of these poles and zeros is as follows: when s equals s_1 or s_3 the value of the numerator of $F(s)$ will be zero and therefore the output of the system will be zero. When s equals s_2 or s_4 the denominator of $F(s)$ will have the value zero and therefore the output of $F(s)$ will be infinite, or said in other words: the system will be unstable.

Taking the log of the latter equation we obtain a formula for the real part of the equation $|F|$ and one for the imaginary part of the formula (the angle (\angle) of F).

$$\log |F| = \log |K_2| + n_0 \log |s| + \sum_i n_i \log |1 - s/s_i| \quad (1a)$$

$$\angle F = \angle K_2 + n_0 \angle s + \sum_i n_i \angle \left(1 - \frac{s}{s_i}\right) \quad (1b)$$

In these formulas, all the variables are real numbers.

By taking the log, we obtain the following advantages: multiplication becomes addition (which is easier to implement given the electronic circuits of those days), we obtain a uniform accuracy over four decades and we will obtain more resolution near "zero".

When looking at figure 4 we find on the right hand side of the machine, a set of controls to set the proper values of the sign of K , n_0 and the proper factoring method).

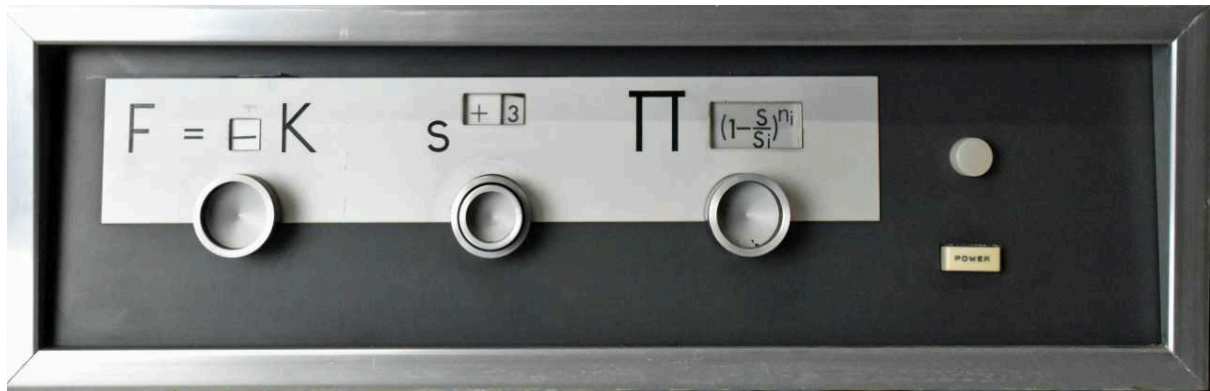


Figure 4 Main control panel for the basic settings of the machine



Figure 5 The plotting area of the Esiac-10

In the middle part of the machine (figure 5), we find the plotting area with the control bar. To the left of the plotting area we see two sliders (potentiometers) marked K and $\angle s$. To the right of the plotting area we find two sliders marked $|F|$ and $\angle F$. Please note the logarithmic scales on some of these sliders and the logarithmic scale on the paper spanning four decades on the X-axis. The vertical (Y) movement of the control bar may be coupled to one of the sliders. The horizontal (X) movement of the control bar is always coupled to s . The precise use of the control bar and the sliders depends upon the calculation to be done and cannot be detailed here.

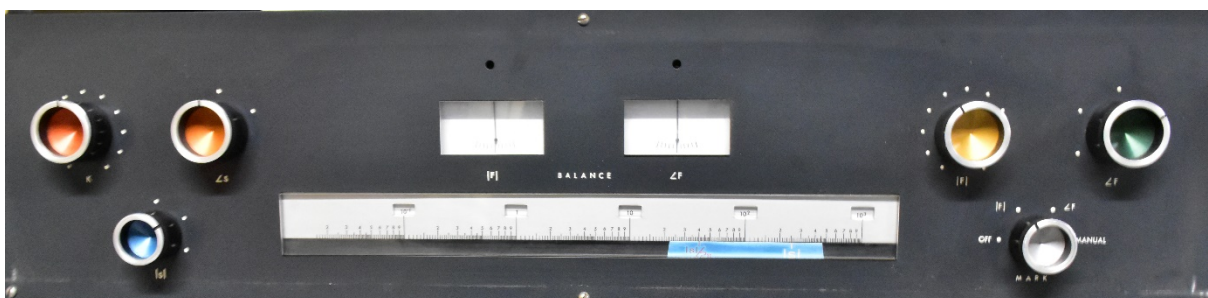


Figure 6 The null-meters, the s -scale and various controls

Two null-balance meters, the s -scale and some switches are located in the panel shown in figure 6. The use of the null-balance meters will be explained later.

To the left and to the right side of the machine there are two grey areas. These areas are two sheets of two dimensional uniform resistance paper. On the left side the magnitude sheet; on the right side the phase sheet. Figure 7 shows how probes sensing the voltage on the phase sheet are coupled to

either the zero or the pole bus bar. These probes are clamped to a moving frame with their tips sliding on the sheets. The probe clamping screw contains a small capacitor representing the exponent n_i . The moving frame can be considered as a coordinate system relative to which the centre of the sheets corresponds to the reading of the $|s|$ and $\angle s$ scales. The frame is constrained to move in translation only, in the manner of a drafting machine, and the $|s|$ and $\angle s$ scales are permanently coupled to its motion.

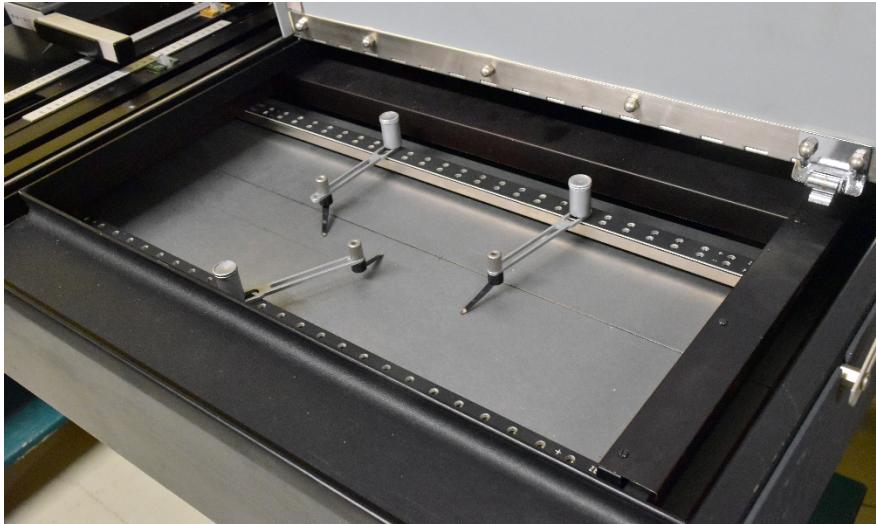


Figure 7 The phase sheet containing three probes

Une Pièce de Résistance

The publication by Sidney Darlington [8] describes how potential analogue planes have been used around 1960 to develop active networks. The important result of the potential analogue planes theory states the following: When electric current flows in a uniform layer or sheet of resistive material, the voltage contours (**equipotential lines**) and the **current streamlines** obey the same geometric laws as the **real** and **imaginary** components of analytic functions of a complex variable.

Complex variables, as present in our calculations can thus be represented by voltages and currents in an isotropic uniform sheet of resistive material. The sheet material used in the ESIAC is so-called Teledeltos paper[9]; visible in figure 7.

Instead of reproducing the potential plane theory, we will suffice here with a simplified example. In figure 8 we have a two dimensional resistance sheet where a current is flowing into the sheet at a point called a sink and (the same) current is flowing out of the sheet at a point called a source. Because of the voltage difference between the sink and the source, a current will flow (the green **current streamlines**) and an electric field will be present (the **equipotential lines** perpendicular to the **current streamlines**). The value of the electric field on any position on the surface can be measured by moving a voltage-sensing probe over the surface. Please note that it is not possible to measure the current streamlines easily.

Une Pièce de Résistance

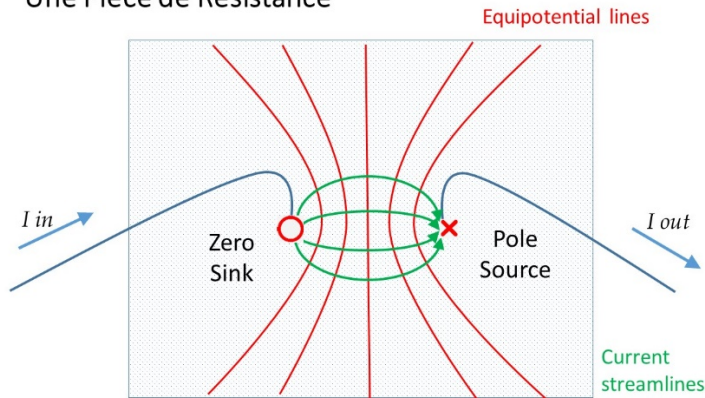


Figure 8 Two-dimensional resistance sheet with a sink and a source

Measuring the current stream lines; introducing dual networks

As said before, it is not possible to measure the current streamlines using a voltage probe. To resolve this problem, an old theorem of electrical theory is used in the ESIAC: Dual Networks (see figure 9 and [11]). In a dual network transformation, a mesh is converted into a node, a resistor into a conductance, a voltage source into a current source and a connection is converted into an open circuit (cut). Figure 10 gives a step-by-step transformation from a Y-circuit containing three inductors to a network containing three capacitors in a delta configuration. Using the duality principle one can thus convert a current measurement into a voltage measurement such that we can measure the phase of equation 1b.

Element	Element
Electrical resistance	Conductance
Inductance	Capacitance
Switch Closed (connection)	Switch Open (isolation)
Mesh	Node

Figure 9 Dual Network transformation

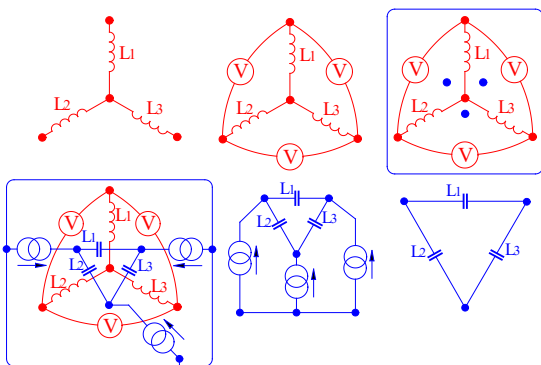


Figure 10 Calculating the dual network - step by step

The duality principle allows us to interchange equipotential lines and current streamlines. Figure 11 gives an explanation for this phenomenon. To explain this, we return to the s-plane. In the same

figure we introduce the finiteness needed to make this principle a workable solution for a measuring instrument. This approximation is allowed when practical sources and sinks use only a small part of the conducting paper.

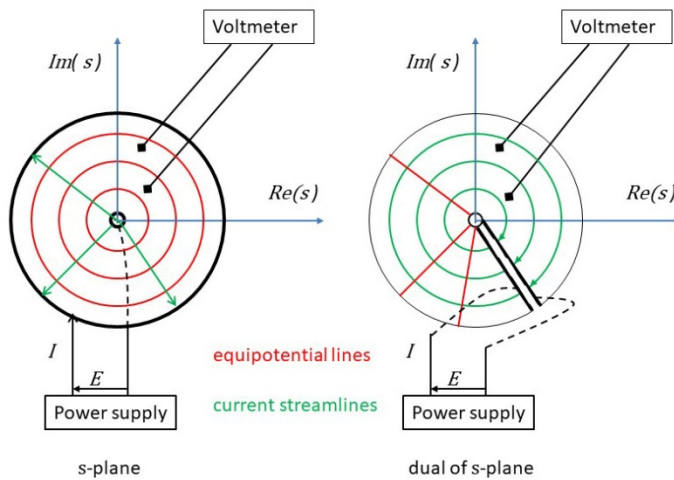


Figure 11 Left- hand side: normal s -plane; right-hand: side the dual of the s -plane.

In the normal s -plane (lhs) the voltage source inserts a current from the source formed by an outer conducting ring into the paper. This current flows to the sink formed by the small inner ring. The reader should study the forms of the equipotential lines and the current streamlines. In the dual of the s -plane (rhs) we want to interchange the equipotential lines and the current streamlines. We need to make an isolating cut in the dual of the s -plane. The reader should again study the forms of both lines. A voltmeter with two probes can be used to measure the potential between any two points on the s -plane. This cut is made always along current streamlines connecting the source and the sink. Whereas the mechanism is clear, it is not easy to extend this to multiple sources and sinks. For each new pair of sources and sinks we would have to make new cuts, which is highly impractical (see [2] for more details).

The reciprocity theorem

The Reciprocity Theorem [10], an old mechanism in electrical engineering, can resolve this problem.

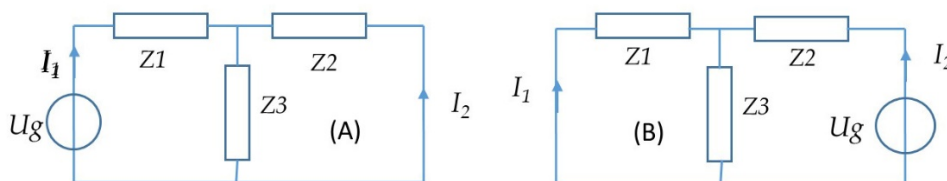


Figure 12 The reciprocity theorem; a simple example

In figure 12 we notice on the left-hand side a simple T-network and a voltage source U_g . Two currents I_1 and I_2 are flowing (System A). By using the Kirchhoff laws one may calculate that it is possible to move the voltage source to another branch of the circuit without any changes in the both currents (System B). The Reciprocity Theorem generalises this result for many voltage sources as follows:

System A which loads currents $I_{n,m}$ in or out at points $s = s_{n,m}$ and where one measures the voltage V_s at single point s may be replaced by System B which loads a single current i_s in or out at point s , and the voltages $V_{n,m}$ are measured at the points $s_{n,m}$. A bit more abstractly, we find the following formula:

$$\sum_n^m i_{n,m} V_s = \sum_n^m V_{n,m} i_s$$

In this way, we are able to replace the set-up with many poles, many zeros and one sensor, by an equivalent network containing a single entry and exit point for the current and a sensor for each of the zeros and poles. That is precisely the set-up shown in figures 8 and 13.

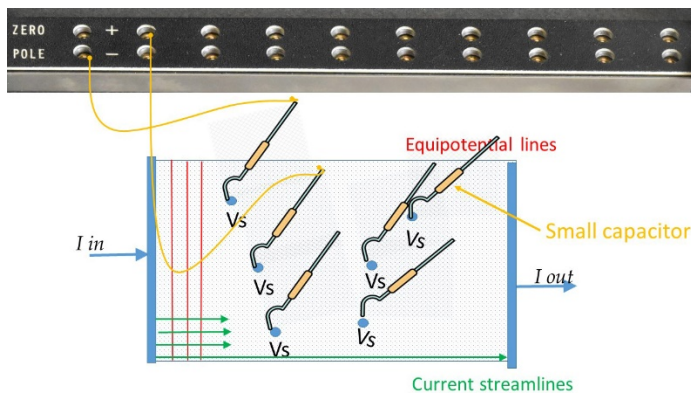


Figure 13 The result of using the Reciprocity Theorem

Now there is one more aspect to take care of: the necessity of the logarithmic scales. Without much explanation, we give the transformation to the $\log s$ scale on the magnitude sheet shown in figure 14.

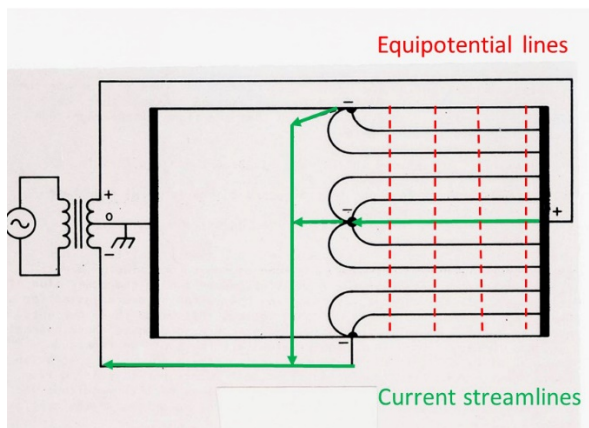


Figure 14 Introducing the $\log s$ scale on the magnitude sheet

Figure 15 shows the complete set-up of both the magnitude and the phase sheets. One can see that a connection in the magnitude sheet corresponds to an open circuit (cut) in the phase sheet etc. It should also be noted that the phase sheet consists of two parts. When measuring phase, one often needs more than a full phase circle and therefore each of the two halves of the phase sheet covers 360° . Also, notice the logarithmic form introduced into the phase sheet.

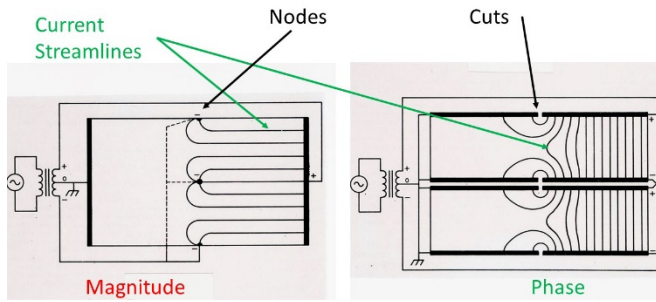


Figure 12 Magnitude and phase sheet of the ESIAC

The electronic details

Figure 16 shows the block diagram of the electronics for the magnitude sheet. First of all, it must be stated that the machine works on alternating current with a frequency of 50 or 60 Hertz. From the block diagram, one may notice that there are two (sets of) probes on the sheet in this example. A (zero) probe is connected to the zeros bus bar; a pole probe is connected to the poles bus bar. Both bus bars are connected to a differential transformer effectively taking the difference of both signals in accordance with formulas 1a and 1b. Additionally, the signal $n_0 \log|s|$ is added to the zeros bus bar and the signal $\log|F| - \log|K|$ is added to the poles bus bar. These signals are generated by the potentiometers next to the plotter. This plotter is by no means an automatic instrument as we are nowadays used to. During a measurement experiment, the user manually operates these potentiometers and the control bar to obtain a null on the balance meters indicating a proper point for plotting has been reached. A similar block diagram exists for the phase-part. Due to space restrictions, this cannot be elaborated here.

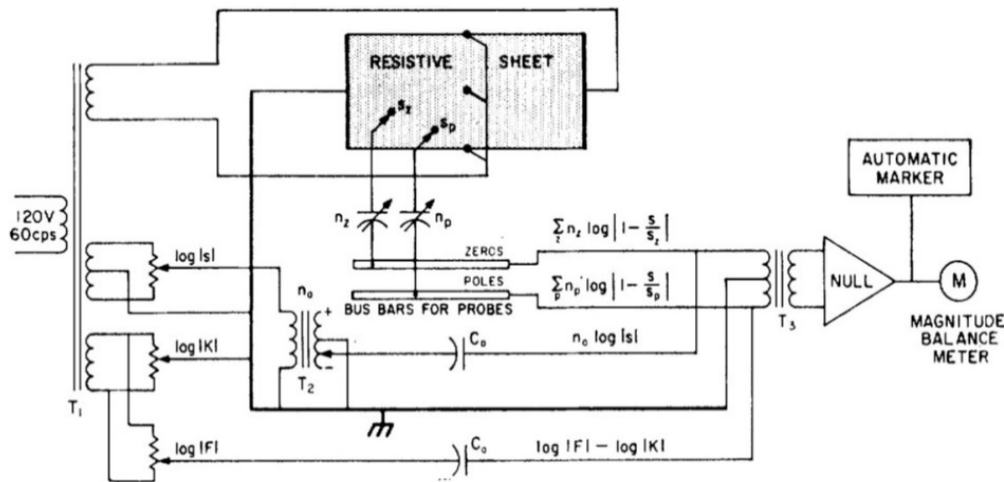


Figure 13 Block diagram of the magnitude part of the electronics

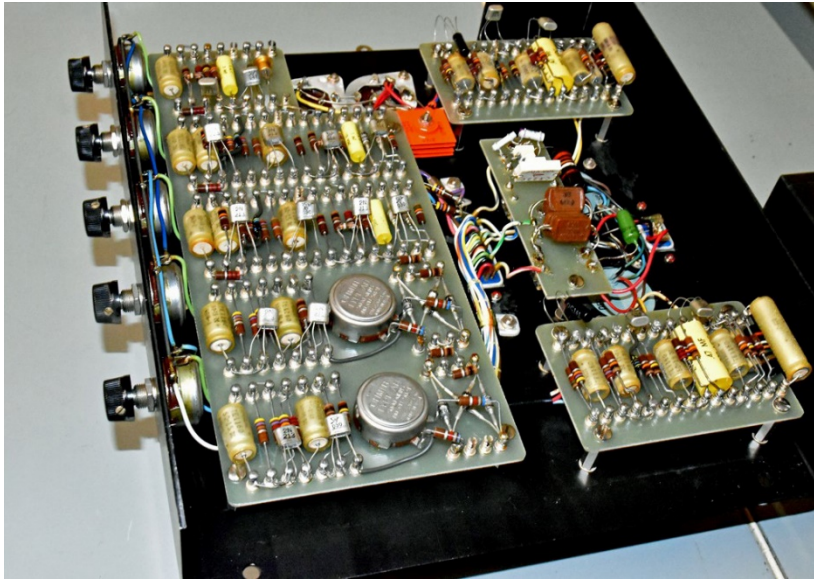


Figure 14 The electronic circuits of the ESIAC

In figure 17 the very modest electronic circuits in the ESIAC are shown. There are two sets of amplifiers (magnitude and phase), some synchronous detectors and a special circuit to take care of phase shifts greater than 360° . The amplifiers are built-up using germanium transistors equivalent to the AC127 as used in Europe.

Conclusion

The ESIAC-10 algebraic computer stands at the intersection of control technology (Bode plots, root-locus plots), theoretical electrical engineering (reciprocity theorem, dual networks) and applied electronics. The machine has been in use at the former electronics department of the TU Delft to study the principles and use of Bode-diagrams and root-locus plots; at that time a new subject developed in the area of control engineering. Apart from the above mentioned purposes of the machine, the ESIAC can be helpful with the factorization of polynomials and residue calculations. The accuracy of the electrical components of the machine is stated to be better than 0.1%. The main source of inaccuracy is the Teledeltos paper which has an accuracy of about 2.5 mm. In [3] it is promised that better resistance sheets are on their way.

This article is based upon a presentation about the principles of the ESIAC-10 algebraic computer given by the first author in October 2021. Currently, we are trying to revive the machine. We retrieved the original service manual [12] and using that, we were able to find a mechanical problem in the machine. Having resolved that problem with the help of other volunteers, we are now striving to bring the machine into working order again. Should we succeed, we will be able to do network calculations such as Bode plots, root-locus plots, transfer functions and residue calculations of dynamic systems in the way envisaged by prof. Huydts around 1965.

The authors want to thank Bernhard Hoenders, Loek van Schie and Otto Rompelman for their help in preparing this material.

Literature

1. Spanning; Geschiedenis van de Delftse opleiding tot elektrotechnisch ingenieur, Jan Davidse, ISBN 90-407-1794-X, 1998, page 85.

2. A Computer for Algebraic Functions of a Complex Variable,
Thesis by M. Loran Morgan (Calif. Institute of Technology 1954, 114 pages).
3. Design of the Esiac® Algebraic Computer,
M. L. Morgan and J. C. Looney,
IEEE transactions on Electronic Computers, Sept. 1961, pp. 524 – 529.
4. A New Computer for Algebraic Functions of a Complex Variable,
M.L. Morgan, IFAC Proceedings, Vol 1, No1 , Aug. 1960.
5. Algebraic Function Calculations Using Potential Analog Pairs,
M. L. Morgan, Proc. of the IRE, 1962, Vol 49, No. 1, pp 276-282.
6. Controls Analysis Of Nuclear Rocket Engine At Power Range Operating Conditions,
Dale J. Arpasi and Clint E. Hart, 1967 (NASA).
7. Frequency Response and Transfer Functions of a Nuclear Rocket Engine System Obtained
from Analog Computer Simulation,
Clint E. Hart and Dale J. Arpasi, NASA, Techn. Note TN D-3979, May 1967.
8. The Potential Analogue Method of Network Synthesis,
Sidney Darlington, Bell System Technical Journal, April 1951, Vol. 30, No 2.
9. Teledeltos paper: <https://en.wikipedia.org/wiki/Teledeltos>
10. Reciprocity and EMC Measurements, Jasper J. Goedbloed, Philips Research, Eindhoven.
11. [https://en.wikipedia.org/wiki/Duality_\(electrical_circuits\)](https://en.wikipedia.org/wiki/Duality_(electrical_circuits))
12. Electro-Scientific Ind., ESIAC Computer Instruction Manual, Model 10, June 1960.